Diagnostic of graphene on Ge(100)/Si(100) in a 200 mm wafer Si technology environment by spectroscopic ellipsometry/reflectometry

Oksana Fursenko, Mindaugas Lukosius, Joachim Bauer, Claus Villringer, Helge Lux, Florian Bärwolf, Marco Lisker, and Andreas Mai

Citation: Journal of Vacuum Science & Technology B **37**, 062927 (2019); doi: 10.1116/1.5122792
View online: https://doi.org/10.1116/1.5122792
View Table of Contents: https://avs.scitation.org/toc/jvb/37/6
Published by the American Vacuum Society

Diagnostic of graphene on Ge(100)/Si(100) in a 200 mm wafer Si technology environment by spectroscopic ellipsometry/reflectometry

Oksana Fursenko,[1,a)] Mindaugas Lukosius,[1] Joachim Bauer,[2] Claus Villringer,[2] Helge Lux,[2] Florian Bärwolf,[1] Marco Lisker,[1] and Andreas Mai[1]
[1]*IHP-Leibniz-Institut für innovative Mikroelektronik, Im Technologiepark 25, 15236 Frankfurt (Oder), Germany*
[2]*Department of Photonics, Laser and Plasma Technologies, Technical University of Applied Sciences Wildau, Hochschulring 1, 15745 Wildau, Germany*

(Received 31 July 2019; accepted 1 November 2019; published 15 November 2019)

Comprehensive diagnostics is a prerequisite for the application of graphene in semiconductor technologies. Here, the authors present long-term investigations of graphene on 200-mm Ge(100)/Si(100) wafers under clean room environmental conditions. Diagnostic of graphene was performed by a fast and nondestructive metrology method based on the combination of spectroscopic ellipsometry and reflectometry (SE/R), realized within a wafer optical metrology tool. A robust procedure for unambiguous thickness monitoring of a multilayer film stack, including graphene, interface layer GeO_x underneath graphene, and surface roughness is developed and applied for process control. The authors found a relationship between the quality of graphene and the growth of GeO_x beneath graphene. Enhanced oxidation of Ge beneath graphene was registered as a long-term process. SE/R measurements were validated and complemented using atomic force microscopy, scanning electron microscopy, Raman spectroscopy, and secondary ion mass spectrometry. This comparative study shows a high potential for optical metrology of graphene deposited on Ge/Si structures, due to its great sensitivity, repeatability, and flexibility, realized in a nondestructive way. *Published by the AVS.* https://doi.org/10.1116/1.5122792

I. INTRODUCTION

Adding graphene to Si-based microelectronic technology enabling its new functionalities is considered a very appealing scenario.[1] However, the formation of carbide during the graphene growth process makes the fabrication of graphene directly on Si wafers extremely challenging. Chemical vapor deposition (CVD) of graphene on transition metals with a following graphene transfer process has been considered a major step toward the commercial realization of graphene. As it was previously reported,[2] graphene transferred from the Cu substrate is associated with a significant risk of metallic contaminations, which prohibits the handling of graphene within a CMOS process line.

Another way to make graphene compatible with Si technology is the graphene transfer process from Ge wafers to various sorts of patterned 200 mm Si wafers on which further process development takes place.[3] The growth technique of high-quality graphene layers by the CVD method on Ge(100)/Si(100) wafers was proposed elsewhere.[3–6] The availability of smooth, more than 2 μm thick Ge(100) epitaxial layers with a low threading dislocation density on Si(100)[7] enables such fabrication of graphene layers. A thick Ge layer can prevent any Si diffusion into the Ge surface at high temperatures.

The transferred graphene films with a large area, clean, and low defect surface are crucial to the performances of microelectronic devices. The stability of graphene up to the beginning of the transfer process is very important. Moreover, storage time in technology can influence the long-term stability of graphene for industrial purposes.

The successful integration of graphene into microelectronic devices depends not only on various technological aspects but also on the availability of fast and nondestructive characterization methods of graphene deposited on large diameter production wafers, which are in the interest of the semiconductor industry. The optical diagnostic of graphene films deposited on substrates other than SiO_2/Si has been a challenging task so far. The use of conventional reflectometry techniques, as it was proposed for exfoliated graphene on SiO_2[8] for films less than 2 nm on bulk substrates, is an insoluble task. Recently, we demonstrated[9] a fast and nondestructive metrology method, which allows one to perform a reliable identification of graphene after the CVD process on 200-mm Ge(100)/Si(100) wafers. The method is based on a combination of UV-Vis spectroscopic ellipsometry and near normal incidence reflectometry (SE/R) with small light spots ($\sim 30 \times 30\,\mu m^2$), realized in a wafer optical metrology tool. A robust procedure for unambiguous thickness monitoring of a multilayer film stack, including graphene, interface layer underneath graphene, and surface roughness is developed and applied for process control of CVD graphene on 200 mm Ge(100)/Si(100) wafers. Based on these results, we report here a long-term stability investigation of graphene on Ge(100)/Si(100) wafers in a clean room environment using the proposed method, which has not been demonstrated so far. The quality of graphene is evaluated by establishing Ge/Si substrate oxidation beneath graphene with the formation of Ge native oxide. SE/R measurements are validated and complemented using atomic force microscopy (AFM),

Note: This paper is part of the Conference Collection: 8th International Conference on Spectroscopic Ellipsometry 2019, ICSE.
[a)]Electronic mail: fursenko@ihp-microelectronics.com

scanning electron microscopy (SEM), Raman spectroscopy, and secondary ion mass spectrometry (SIMS).

II. EXPERIMENT

Graphene was deposited by CVD on 200-mm Ge(100)/Si(100) wafers in an Aixtron's Black Magic BM300T CVD tool at 885 °C using CH_4 as the carbon source and Ar/H_2 mixture as the carrier gas. The pressure of 700 mbar was kept constant during the depositions. The optimized deposition time was 60 min. The details of the growth of these films are already published.[6–7] Epitaxial Ge(100) with a low threading dislocation density (below 1×10^8 cm^{-2}) and low surface roughness, deposited by reduced pressure chemical vapor deposition[7] on Si(100) wafers, was used as a substrate.

The long-term stability of graphene on Ge(100)/Si(100) wafers, stored in a clean room environment at room temperature, has been routinely monitored performing continuous measurements over a period of more than 2 years using a combination of spectroscopic ellipsometry and reflectometry. Thickness monitoring was performed on a KLA-Tencor SpectraFx200 wafer metrology tool in the wavelength range of 240–800 nm using ellipsometry setup with an ~71° angle of incidence (AOI) and in the wavelength range of 190–300 nm using 63° AOI and near normal incidence reflectometry setup with small spot objectives (30–40 μm).

Raman spectroscopy was applied for graphene quality and layer strain evaluation. The measurements were realized using a WiTec alpha 300 micro-Raman microscope with 488 nm excitation laser wavelength with 30 mW power and a lens magnification of 50× (spot size: ~0.5 μm).

AFM with a Park NX20 system and SEM measurements were performed for microtopography evaluation. The macroimages with a scan size of $30 \times 30\,\mu m^2$ additionally to microimages of $2 \times 2\,\mu m^2$ were monitored for compatibility with an illumination spot of optical wafer metrology tool.

SIMS was used for a direct analysis of the surface and interfacial compositions. Measurements were carried out on CAMECA IMS Wf. In order to reach maximum sensitivity for the $^{12}C^-$, $^{18}O^-$, and $^{70}Ge^-$ isotopes, the tool was tuned for cesium sputtering at 440 eV impact energy in the negative mode. Current density was chosen to be as low as possible to further increase the depth resolution. All measurements were done within one cycle to minimize parameter drift and to allow a direct comparison to each other.

III. RESULTS

A. Spectroscopic ellipsometry and reflectometry

Some selected SE/R experimental results of monitoring of graphene on Ge(100)/Si(100) wafer over the period of ~2.5 years are displayed in Fig. 1. It is possible to observe the systematical changes in all optical quantities (reflection, $\tan\Psi$, $\cos\Delta$) during the wafer aging. The greatest changes are visual in the full wavelength range for $\cos\Delta$, which is a phase quantity and is extremely sensitive to very thin films. Considering the measurements of a bare Ge wafer with native oxide (1.1 nm) before graphene deposition and 1 month after graphene deposition, it is possible to observe similar differences compared to the wafer just after graphene deposition. All optical quantities show similar systematical shifts within the aging time. The observed changes in the spectra cannot be addressed to the graphene layer modification due to its relatively low contribution to the optical quantities.[9] That is, the optical measurements reveal another layer formation. Considering the influence of GeO_2 on the optical responses (sensitivity plots), calculated for graphene(0.3 nm)/GeO_2(1.5 nm)/Ge film stack [Figs. 2(d)–2(f)], we concluded GeO_x growth beneath graphene.

The sensitivity plots of optical quantities to graphene and GeO_2 layer thickness for the graphene(0.3 nm)/GeO_2(1.5 nm)/Ge stack were calculated and are shown in Fig. 2. The structure model for SE/R simulations, consisting of the Ge substrate, an interlayer of native oxide (GeO_2), which is typically present on the surface of Ge and indirectly included the interface roughness, and the deposited layer of graphene, was used. Optical constants for graphene were accurately determined on SiO_2/Si substrates using broadband multiangle reflectometry-ellipsometry techniques.[9] Optical parameters for Ge and GeO_2 were taken from a recent investigation.[10] All layers were treated isotropically. Si was not included in the optical model due to the relatively thick Ge layer above, which is considered bulk within the UV-Vis spectral range.

The sensitivity of ellipsometry measurements to monolayer graphene [Figs. 2(a) and 2(b)] is shown in the responses of both $\tan\Psi$ and $\cos\Delta$ for AOI ≈ 71°. In the case of AOI ≈ 63°, the overall sensitivity is lower, but $\tan\Psi$ shows still significant changes in the 250–300 nm range. Maximum sensitivity of the spectroscopic ellipsometry setup is observed in the ultraviolet region of the spectrum (250–400 nm), where a strong peak of the extinction coefficient of graphene (Van Hove singularity and excitonic effect) is identified and a difference up to 2.0% between the bare substrate and graphene on the substrate is observed. The change in Δ is about 1.5° at 300 nm for the graphene monolayer and over an order of magnitude higher than the sensitivity limit of the tool (~0.02°). Additionally, the 600–800 nm wavelength range can improve the sensitivity for graphene monolayer identification where a higher sensitivity of $\tan\Psi$ is observed. Such sensitivity makes graphene surely detectable and measurable on Ge/Si substrates. Therefore, an ellipsometry setup is a suitable choice for graphene layer evaluation for the considered film stack, and all thicknesses can be reliably quantified.

Considering the reflection sensitivity plot [Fig. 2(c)], we can conclude that reflectometry alone cannot provide enough sensitivity for an adequate determination of monolayer graphene. The sensitivity to the graphene monolayer is quite small and only visible in the UV range, where the surface roughness has a similar effect on the reflection. As we have shown recently,[9] reflectometry measurements can be applied for surface roughness evaluation.

Choosing the best experimental conditions, prior to experiments, seems to be a useful process. Considering the sensitivity plots of optical responses to graphene and GeO_2 for the graphene/GeO_2/Ge stack over the area of measured

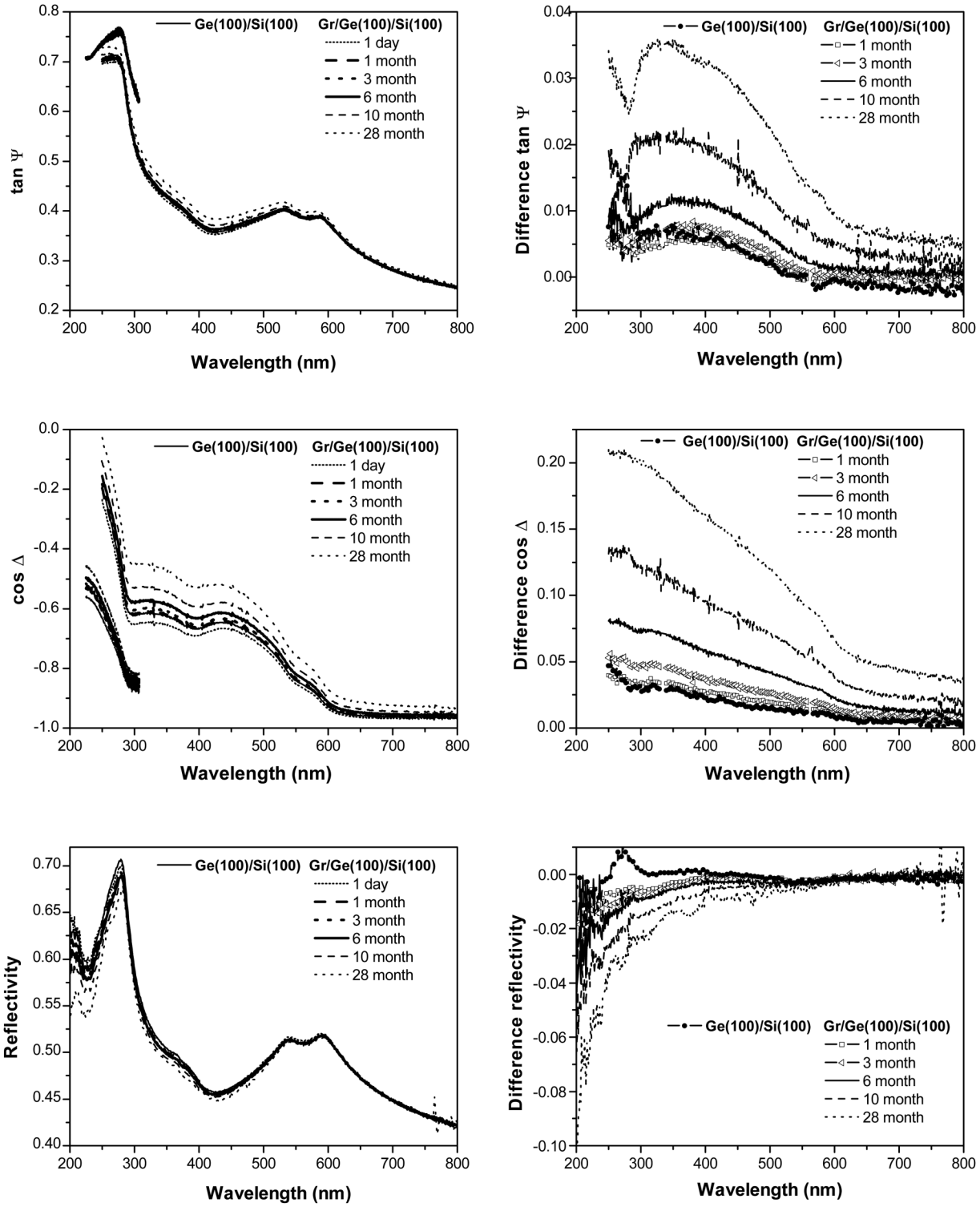

FIG. 1. Experimental tan Ψ, cos Δ (AOI = 63°, 71°), and reflectivity measurements performed on bare and graphene (Gr) covered Ge(100)/Si(100) wafers over the storage time (1 day, 1, 3, 6, 10, and 28 months after deposition) and corresponding differences to 1 day storage wafer.

wavelength and angles of incidence (Fig. 2), it is possible to conclude that the best experimental conditions for the diagnostics of these layers are near Brewster or principal angle for Ge (AOI ~ 80°). The multiangle-range of measurements is the preferred method to receive the layers' parameters. Nevertheless, this type of measurement is not always possible, particularly when wafer metrology tools are used. For these tools, AOI ≤ 70° are the source of limitations for the small spot size of the ellipsometer.

B. Atomic force microscopy and scanning electron microscopy

The optical quantities (reflection, ellipsometric ratio, and scattering) of randomly rough surfaces generally depend on

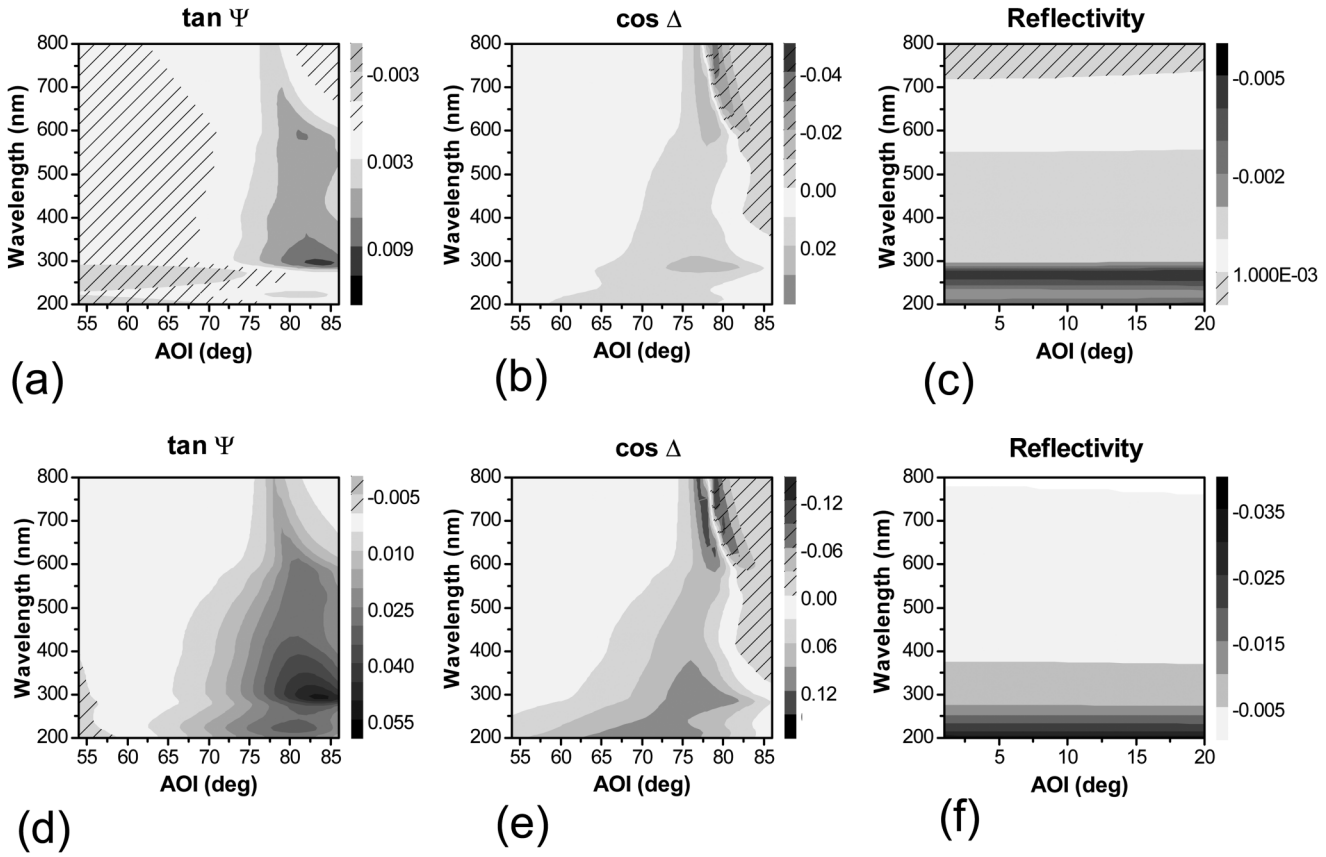

FIG. 2. Sensitivity of tan Ψ [(a) and (d)], cos Δ [(b) and (e)], and reflectivity [(c) and (f)] over area of wavelength and AOI to monolayer graphene (0.3 nm) [(a)–(c)] and GeO_2 (1.5 nm) [(d)–(f)] for the graphene(0.3 nm)/GeO_2(1.5 nm)/Ge stack.

vertical and lateral dimensions of the surface irregularities. The evolution of the surface topography over time is analyzed by AFM and SEM. Figure 3 shows AFM images of the graphene/Ge(100)/Si(100) surface after graphene deposition (a) and 2.5 years (b) aging in air with $2 \times 2\,\mu m^2$ and $30 \times 30\,\mu m^2$ scan sizes.

The AFM and SEM topography scans of $2 \times 2\,\mu m^2$ for graphene after deposition [Figs. 3(a) and 4(a)] show that the graphene-induced Ge faceting is clearly recognizable as hill-and-valley structures with fourfold symmetry of patterns and a root mean square (RMS) roughness σ of ~1 nm ($2 \times 2\,\mu m^2$) and ~2 nm ($30 \times 30\,\mu m^2$). After graphene deposition, RMS σ is increased in comparison to bare Ge(100)/Si(100) wafers, where $\sigma \sim 0.13$ nm and ~0.8 nm, correspondingly, were measured.[9]

The dimensions of the faceted structures visible in AFM images are typically less than 2 nm height and nearly 100 nm wide. The formation of Ge facets during graphene growth by CVD was reported previously.[11] These Ge facets formed at elevated temperatures and are stable under ambient conditions. This is a result of the mismatch of the thermal expansion coefficient between graphene and Ge when rapidly cooling the wafer to room temperature. At lower temperatures, the germanium diffusion length during the cooling period is short, leading to the formation of terraces rather than to a planar (001) surface. Different Ge faceting modifications can be observed with a different cooling rate.

After aging the wafer, we have observed a modification of the surface structure [Figs. 3(b) and 4(b)]: some domains without faceting increased in size over time to one close surface. A slight increase of the root mean squared surface roughness from $\sigma \sim 1.0$ to 1.3 nm for microscans is observed too, after the storage of graphene over the whole investigated time. For $30 \times 30\,\mu m^2$ macroscans, the roughness σ was measured near the same ~2 nm.

As we have shown,[9] for the graphene faceting structures where $\sigma \ll \lambda$, the scattering effect can be neglected and the optical measurements provide the averaged area information (~$30 \times 30\,\mu m^2$), without a high spatial resolution. The main spatial wavelength interval, which describes the periodical part of the surface roughness or autocorrelation length $L_c \sim 0.7 \pm 0.16\,\mu m$ is comparable with the wavelength of the incident light. In such a case, the effect of surface roughness has the most impact on reflectometry. The reason for this is the low scattering associated with a relatively low roughness. At the same time, such a surface roughness has no influence on the ellipsometry measurements for the graphene monolayer on GeO_2/Ge, as it has also been demonstrated by rigorous coupled wave analysis simulations.[9]

C. Raman spectroscopy

Figure 5 shows the Raman spectra of graphene on Ge(100)/Si(100) after 1 week and 2.5 years wafer storage

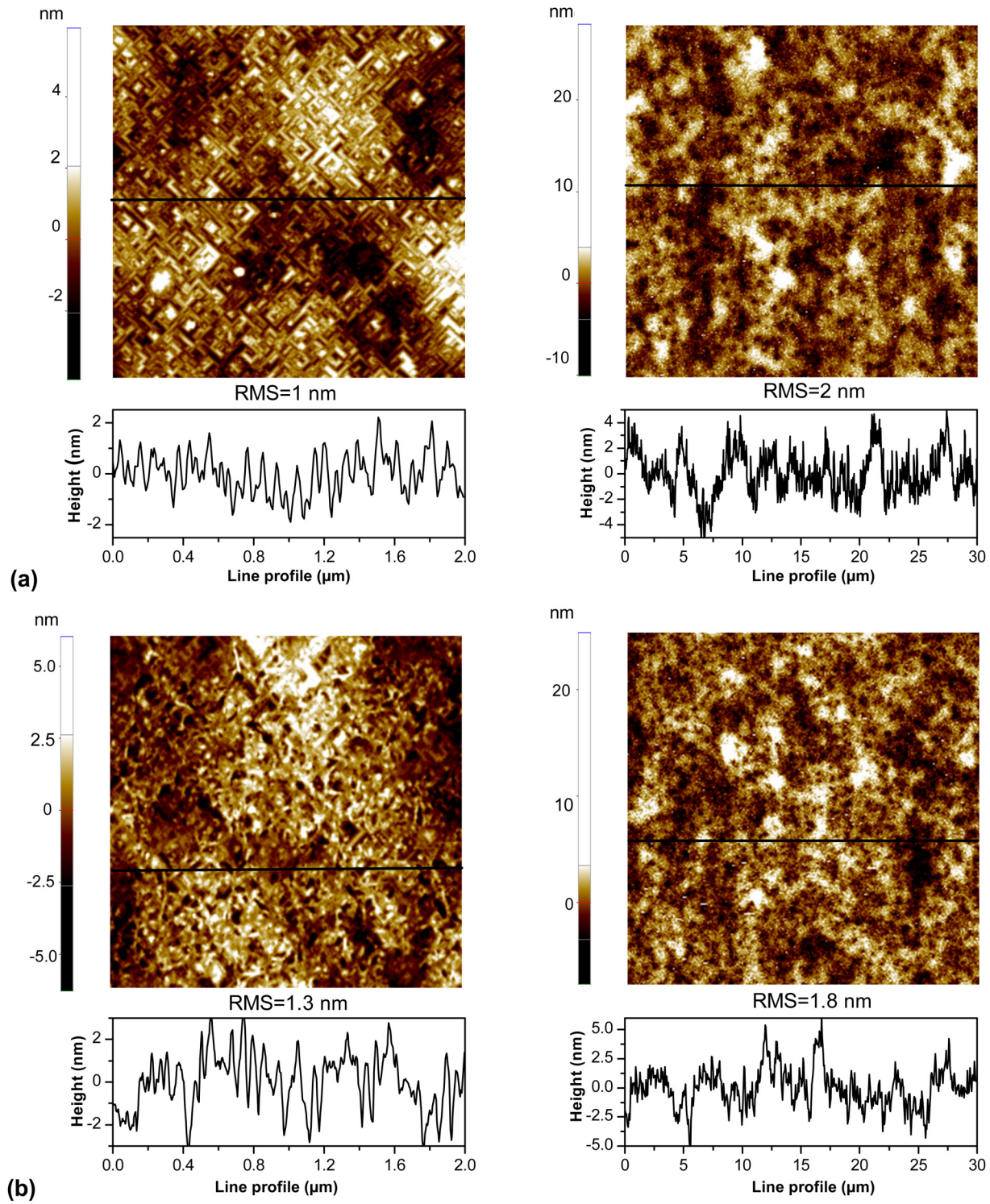

FIG. 3. AFM topography images (2×2 and $30 \times 30\,\mu m^2$) with surface roughness RMS and line profiles of graphene on Ge(100)/Si(100) wafers after graphene deposition (a) and 2.5 years (b) aging in a clean room environment.

with its characteristic G at $\sim 1580\,cm^{-1}$, 2D at $\sim 2700\,cm^{-1}$, and D at $\sim 1350\,cm^{-1}$ peaks of graphene. It is possible to observe that after 2.5 years aging, there are substantial differences in the D, G, and 2D bands. The observed downshifts in the G band and 2D band (average shift, $\sim 7\,cm^{-1}$) can be attributed to the tensile biaxial strain of graphene, probably caused by bond stretching and lattice distortion due to GeO_x formation.[12] The existence of the D peak after 1 week aging is direct evidence for the existence of point defects or grain boundaries, as the means of access for oxidizing agents to the interface. Increasing the D peak with the aging time implies the formation of new defects within the graphene layer. The Raman I_D/I_G ratio increased throughout the Ge oxidation

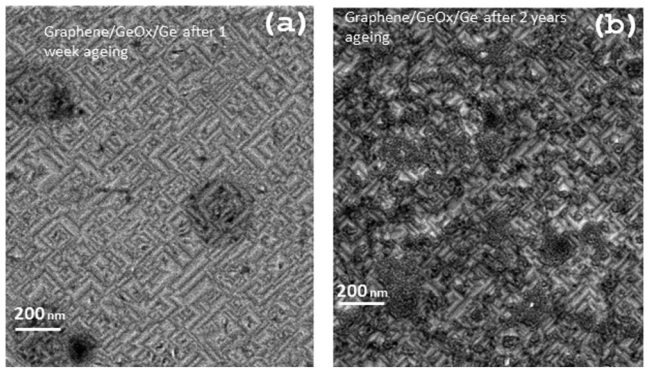

FIG. 4. SEM topography images of graphene on Ge(100)/Si(100) wafers after 1 week (a) and 2.5 years (b) aging in a clean room environment.

process, suggesting that the graphene defect density is increased.

D. Secondary ion mass spectrometry

Oxide formation beneath graphene was verified by SIMS measurements of bare Ge(100)/Si(100) and graphene-covered Ge(100)/Si(100) wafers after storing them both for over 2.5 years. As seen in Fig. 6, both the bare and graphene-covered samples exhibit similar oxygen $18O^-$ and germanium $70Ge^-$ peaks, but enhanced Ge oxidation in the presence of graphene is observed.

The $70Ge^-$ signal was chosen as reference and is perfectly overlapping from one sample to another. This means there is nearly no drift of parameters within the measurement settings. These ideal conditions are necessary for comparing raw data SIMS signals. Sputter equilibrium for a bare sample is reached after ~200 s and for the graphene-covered sample after ~300 s sputter time. This indicates a much thicker surface layer for the graphene-covered sample.

It is difficult to pinpoint an exact position of the oxygen or carbon layer, because of the atom mixing during the sputtering process, which is an inherent measurement property. Choosing low impact energy, we minimized this knock-on effect. The oxygen content additionally changes the secondary ion yield for all elements, which leads to a change of signal intensities for $12C^-$ and $70Ge^-$. From the peak positions of the $12C^-$ and $18O^-$, it is possible to argue with causality. This means that in the case of the graphene-covered sample, the oxygen layer is beneath the carbon layer. In the case of the bare sample, the carbon surface peak is broadened and its peak position is beneath the oxygen layer. Its relatively low intensity additionally shows that this is just adventitious carbon.

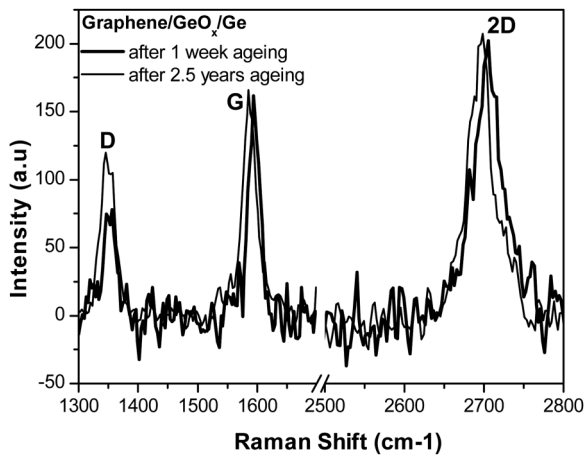

FIG. 5. Averaged Raman spectra from large area scan, showing characteristic G, 2D, and D bands of graphene on Ge(100)/Si(100) after 1 week and 2.5 years' aging. Graphene defects development after 2.5 years storage in air (D peak) and strain induced Raman G and 2D peak shifts, caused by bond stretching and lattice distortion.

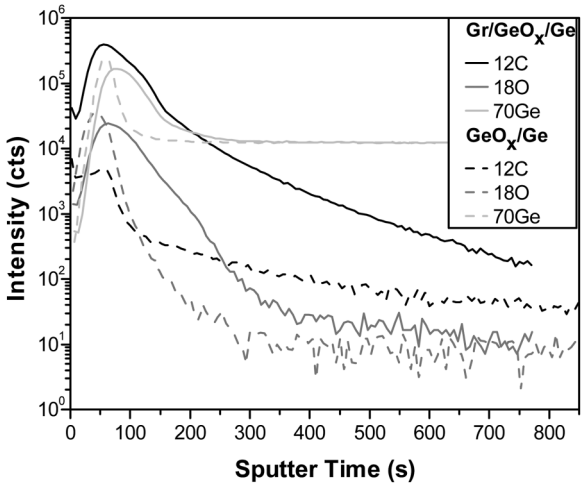

FIG. 6. Intensity over sputter time profiles of Ge(100)/Si(100) wafers with (bold lines) and without (dashed lines) graphene (Gr) after 2.5 years aging in air.

IV. DISCUSSION

The oxidation behavior of germanium underneath graphene is scarcely reported. It was published[13] that the growth of graphene on Ge(100) produces excellent passivation of Ge with the protection from oxidation on a time scale of at

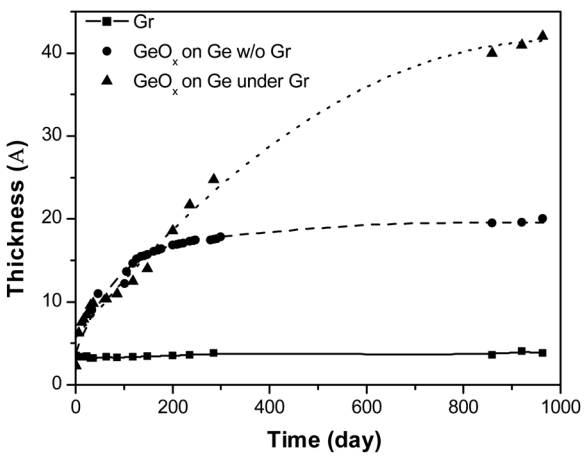

FIG. 7. Thickness of graphene (Gr) and GeO_x on Ge(100)/Si(100) wafers with and without graphene over time of aging. Wafers were stored in a clean room environment.

least months. However, Jacobberger *et al.*[14] demonstrated that the passivation of germanium is a complicated process, and several factors like process parameters and Ge surface orientation govern the oxidation of Ge coated with graphene. It was found that Ge(110) oxidizes significantly less than Ge(100) or Ge(111) after 1 month of air exposure, even at the same graphene defect density. Our detailed investigation of the long-term stability of CVD graphene on Ge(100)/Si(100) wafers shows a significant and rapid oxidation behavior: we have observed GeO_x formation on Ge under graphene from environment absorbed agents by different methods. One possible explanation of GeO_x observation could be that the oxidation of Ge resulted in a change of surface topography after graphene deposition and the creation of faceting structures with well-organized hill and valley structures. These structures can tune the catalytic

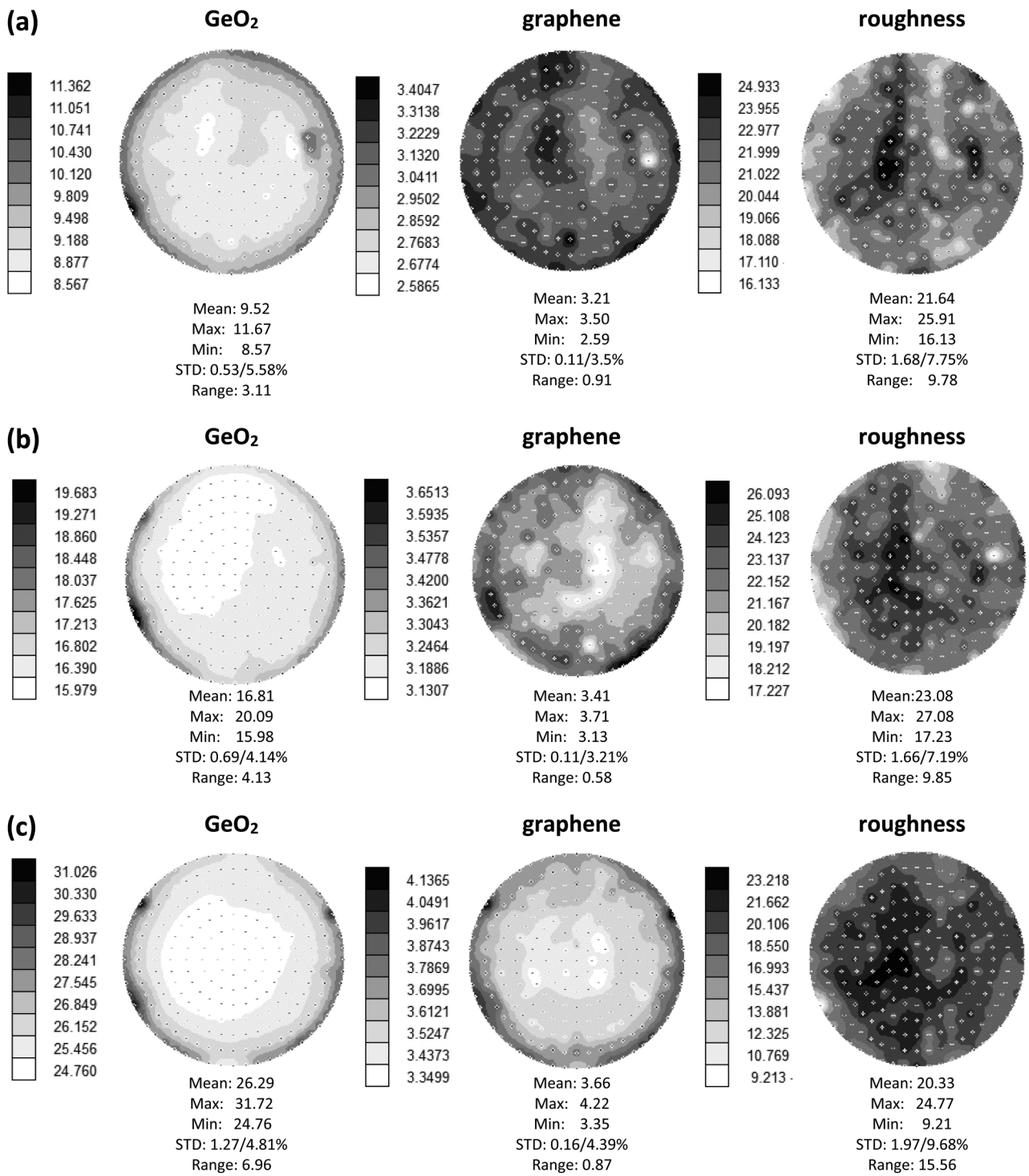

FIG. 8. Thickness (in angstroms) of GeO_2, graphene, and surface roughness for graphene/GeO_2/Ge(100)/Si(100) 200-mm wafers after 1 (a), 7 (b), and 11 months (c) aging in room temperature conditions, performed by SE/R. The marked sites correspond to the measurement positions.

oxidation activity and enhance the defect generation. According to Ref. 15, nonuniform graphene with weaker graphene-Ge interactions on top of the nanofacets, which resulted in high-quality graphene and graphene with lower quality in the valley regions of the nanofacets, due to the stronger graphene-Ge interactions, is generated. We suppose that oxidation beneath graphene resulted from microscopic defects or grain boundary caused the faceting structure of germanium with the formation of locally oxidized domains. The oxidized domains seem to increase in size over time to one common closed GeO_x film. It is reasonable to assume that larger density of defects for the graphene coating will induce a faster oxidation of the Ge underneath, as it was already observed on copper surfaces.[16,17] The preparation of the Ge surface is a crucial factor in determining the properties of the graphene layer, as it is already mentioned.[17]

The degree of oxidation SE/R measurements were carried out continuously with respect to quantification. The calculated thickness values for two Ge(100)/Si(100) wafers, uncoated and coated with graphene, are shown in Fig. 7. The structural model is built up from the substrate (Ge), an interface layer (GeO_2), and the graphene layer. Surface roughness modeling was implemented in the KLA-TENCOR software, based on the scalar diffraction theory. The parameters of graphene, GeO_2 layer thickness, and surface roughness were fitted until the experimental and calculated data matched. Excellent agreement between experimental and best-match calculated $\tan\Psi$, $\cos\Delta$, and reflectivity is achieved with more than 0.85 goodness of fit (GOF). GOF is used in the industry based on chi-squared biased estimator calculations. The results of the calculation of the correlation matrix of fit parameters show that the correlation between GeO_2 and graphene layer thickness is in the range of 0.6–0.8; at the same time, the correlation of these parameters to the roughness is near 0. That is why combined data collection (ellipsometry and reflectometry) facilitates unambiguous identification of graphene and GeO_2 on Ge for complex evaluation of a graphene layer stack, including surface roughness.

Considering the nonhomogeneous characteristic of Ge oxidation beneath graphene, SE/R measurements unfold the effective layer GeO_2 thickness. We observed that in the first ~200 days aging, the graphene-coated and the bare Ge(100)/Si(100) wafers show similar oxide growth behavior. However, subsequently, a different growth contour is monitored: the graphene-coated wafer underwent more severe oxidation than the uncoated one. The GeO_x thickness growth with a ratio of ~2:1 is observed after 2 years room temperature oxidation of Ge(100) beneath graphene in comparison with uncovered Ge(100). SIMS supports our conclusion that graphene accelerates long-term oxidation of underlying Ge substrate in ambient atmosphere at room temperature. Further investigations of different wafers with deposited graphene monolayers revealed that within a relatively short period of time, the growth of oxide layer occurs with variable thickness values, depending on the quality of the deposited graphene. Thus, the rate of Ge(100) oxidation beneath graphene is different and depends on the quality of graphene layers. Therefore, the SE/R is a powerful application for diagnostics of the quality of graphene on Ge/Si wafers.

Figure 8 shows the maps of 225 points for the thickness of graphene, GeO_2, and surface roughness in ~1, 7, and 11 months after graphene deposition performed by SE/R. The measured average thickness of the graphene layer is in the range of ~0.32–0.34 nm with a standard deviation value (STD) of 3.5%–4.4% over the full wafer and evaluation time. RMS σ is in the range of 2.0–2.3 nm with STD = 7.2%–9.7% and correlates well with AFM measurements. Optical monitoring of the graphene thickness over the whole wafer shows excellent long-term stability ($s = 0.004$ nm) over the evaluation time, independent on the growth of interfacial GeO_2 and surface roughness. GeO_2 thickness growth beneath graphene shows the typical distribution for native oxide over the whole wafer.

Figures 7 and 8 demonstrate a series of results of long-term investigations of graphene on Ge(100)/Si(100) wafers, which can be varied in dependence on the quality of graphene. This implies a problem for the future transfer process of graphene from Ge(100)/Si(100). The proposed method of quality diagnostic of graphene can be applied for other Ge surface orientations also.

V. CONCLUSIONS

In this paper, we have shown the application of spectroscopic ellipsometry/reflectometry for quality diagnostics of graphene on Ge(100)/Si(100) in a 200 mm wafer Si technology environment. This fast and nondestructive method is based on a combination of UV-Vis spectroscopic ellipsometry and near normal incidence reflectometry with a small light spot ($\sim 30 \times 30\,\mu m^2$), realized in a wafer optical metrology tool. A robust procedure for unambiguous thickness monitoring of all components of a multilayer film stack, including graphene, interface layer GeO_x underneath graphene, and surface roughness is developed and applied for process control of CVD graphene on 200 mm Ge(100)/Si(100) wafers.

The results allow the conclusion that the quality of graphene is assessed by the presence of GeO_x beneath graphene. Graphene defects intensified by the facet formation and degradation of Ge, which are created during the graphene CVD process on Ge (100)/Si(100) and allow the local oxidation.

The quality of graphene was evaluated by performing a long-term stability test in a clean room environment over 2.5 years. The oxidation enhancement of Ge under graphene in comparison with uncovered Ge was registered as a long-term process. This effect may be an indicator of potential stability problems for future use of graphene from Ge(100)/Si(100) wafers for transfer processes.

SE/R measurements were validated and complemented using AFM, SEM, Raman spectroscopy, and SIMS. Compared to other methods, the use of optical methods for diagnostics promises to be more flexible, economical, repeatable, effective, and practical realized by a nondestructive way.

[1]M. Lisker *et al.*, Microelectron. Eng. **205**, 44 (2018).
[2]G. Lupina *et al.*, ACS Nano **101**, 4776 (2015).

[3]M. Lukosius *et al.*, ACS Appl. Mater. Inter. **8**, 33786 (2016).
[4]I. Pasternak, M. Wesolowski, I. Jozwik, M. Lukosius, G. Lupina, P. Dabrowski, J. Baranowski, and W. Strupinski, Sci. Rep. **6**, 21773 (2016).
[5]I. Pasternak, P. Dabrowski, P. Ciepielewski, V. Kolkovsky, Z. Klusek, J. M. Baranowski, and W. Strupinski, Nanoscale **8**, 11241 (2016).
[6]G. Lupina *et al.*, ECS J. Solid State Sci. **6**, M55 (2017).
[7]Y. Yamamoto, P. Zaumseil, T. Arguirov, M. Kittler, and B. Tillack, Solid State Electron. **60**, 2 (2011).
[8]A. Gray, M. Balooch, S. Allegret, S. De Gendt, and Wang Wei-E, J. Appl. Phys. **104**, 053109 (2008).
[9]O. Fursenko, M. Lukosius, G. Lupina, J. Bauer, C. Villringer, and A. Mai, Proc. SPIE **10330**, 1033017 (2017).
[10]T. N. Nunley, N. S. Fernande, N. Samarasingha, J. M. Moya, V. M. Nelson, A. A. Medina, and S. Zollner, J. Vac. Sci. Technol. B **34**, 061205 (2016).
[11]K. M. McElhinny, R. M. Jacobberger, A. J. Zaug, M. S. Arnold, and P. G. Evans, Surf. Sci. **647**, 90 (2016).
[12]H. Mi, Zh. Ma, and J. P. Blanchard, "Raman spectroscopy for monitoring strain on graphene and oxidation corrosion on nuclear claddings," in *Raman Spectroscopy and Applications*, edited by K. Maaz (IntechOpen, London, 2017), pp. 123–142.
[13]R. Rojas Delgado, R. M. Jacobberger, S. Singha Roy, V. Saradhi Mangu, M. S. Arnold, F. Cavallo, and M. G. Lagally, ACS Appl. Mater. Interfaces **9**, 17629 (2017).
[14]R. M. Jacobberger, M. J. Dodd, M. Zamiri, A. J. Way, M. S. Arnold, and M. G. Lagally, ACS Appl. Nano Mater. **2**, 4313 (2019).
[15]P. Dabrovski *et al.*, Nano Res. **10**, 3648 (2017).
[16]F. Zhou, Zh. Li, G. J. Shenoy, L. Li, and H. Liu, ACS Nano **7**, 6939 (2013).
[17]M. Schriver, W. Regan, W. J. Gannett, A. M. Zaniewski, M. F. Crommie, and A. Zettl, ACS Nano **7**, 5763 (2013).